Dynamic Modeling and Flight Control Simulation of a Large Flexible Launch Vehicle

Conference Paper · August 2008

DOI: 10.2514/6.2008-6620

3 authors, including:

Bong Wie
Iowa State University
209 PUBLICATIONS **7,269** CITATIONS
SEE PROFILE

Mark Whorton
Teledyne Brown Engineering
60 PUBLICATIONS **714** CITATIONS
SEE PROFILE

AIAA Guidance, Navigation and Control Conference and Exhibit
18 - 21 August 2008, Honolulu, Hawaii

AIAA 2008-6620

Dynamic Modeling and Flight Control Simulation of a Large Flexible Launch Vehicle

Wei Du* and Bong Wie†
Iowa State University, Ames, IA 50011-2271
Mark Whorton‡
NASA Marshall Space Flight Center, Huntsville, AL 35812

This paper presents the preliminary study results of dynamic modeling and flight control simulation of large flexible launch vehicles such as the Ares-I Crew Launch Vehicle. A complete set of six-degrees-of-freedom dynamic models of the Ares-I, incorporating its propulsion, aerodynamics, guidance and control, and structural flexibility, is developed. NASA's Ares-I reference model and the SAVANT Simulink-based program are utilized to develop a Matlab-based simulation and linearization tool for an independent validation of the performance and stability of the ascent flight control system of the Ares-I. A linearized state-space model as well as a non-minimum-phase transfer function model (which is of typical for flexible vehicles with non-collocated actuators and sensors) is validated for the ascent flight control design and analysis of the Ares-I.

Nomenclature

a	speed of sound (= 1117 ft/s at sea level in the standard atmosphere)
b	reference body length = 12.16 ft
(c_x, c_y, c_z)	components of the center of gravity location in the structure reference frame with its origin at the top of vehicle = $(220.31, 0.02, 0.01)$ ft at $t = 0$
C_A	axial force coefficient
$C_{Y\beta}$	side force curve slope with respect to β
C_{N0}	normal force coefficient at zero angle of attack
$C_{N\alpha}$	normal force curve slope with respect to α
$C_{Mr\beta}$	rolling moment curve slope with respect to β
C_{Mp0}	pitching moment coefficient at zero angle of attack
$C_{Mp\alpha}$	pitching moment curve slope with respect to α
$C_{My\beta}$	yawing moment curve slope with respect to β
$\boldsymbol{C}^{B/I}$	direction cosine matrix of the frame B with respect to the frame I
$\boldsymbol{C}^{B/S}$	direction cosine matrix of the frame B with respect to the frame S
C	lateral (side) force
D	drag (axial) force
F_{base}	base drag force
$(F_{aero.xb}, F_{aero.yb}, F_{aero.zb})$	body-axis components of aerodynamic force
$(F_{rkt.xb}, F_{rkt.yb}, F_{rkt.zb})$	body-axis components of solid rocket booster force
$(F_{rcs.xb}, F_{rcs.yb}, F_{rcs.zb})$	body-axis components of RCS force
$(F_{total.xb}, F_{total.yb}, F_{total.zb})$	body-axis components of total force
$(F_{total.xi}, F_{total.yi}, F_{total.zi})$	inertial components of total force
(g_x, g_y, g_z)	inertial components of the gravitational acceleration

*Ph.D. Student, Space Systems and Control Laboratory, Department of Aerospace Engineering, weid@iastate.edu, Student Member AIAA.
†Vance Coffman Endowed Chair Professor, Space Systems and Control Laboratory, Department of Aerospace Engineering, 2271 Howe Hall, Room 2355, (515) 294-3124, bongwie@iastate.edu, Associate Fellow AIAA.
‡Chief, Guidance Navigation and Mission Analysis Branch, mark.whorton@nasa.gov, Associate Fellow AIAA.

$(\vec{i}, \vec{j}, \vec{k})$	basis vectors of the body-fixed reference frame B
$(\vec{i}_s, \vec{j}_s, \vec{k}_s)$	basis vectors of the structure reference frame S
$(\vec{I}, \vec{J}, \vec{K})$	basis vectors of the Earth-centered inertial reference frame I
$(\vec{I}_e, \vec{J}_e, \vec{K}_e)$	basis vectors of the Earth-fixed equatorial rotating reference frame E
J_2	Earth's second order zonal coefficient = 1.082631×10^{-3}
J_3	Earth's third order zonal coefficient = -2.55×10^{-6}
J_4	Earth's fourth order zonal coefficient = -1.61×10^{-6}
$(K_p,\ K_i,\ K_d)$	proportional, integral, and derivative gains of a PID controller
m	vehicle's mass
M	Mach number
N	normal force
p_0	local atmospheric pressure
(p, q, r)	body-axis components of $\vec{\omega}$
(q_1, q_2, q_3, q_4)	attitude quaternions
$(q_{1c}, q_{2c}, q_{3c}, q_{4c})$	commanded attitude quaternions
$(q_{1e}, q_{2e}, q_{3e}, q_{4e})$	attitude-error quaternions
Q	dynamic pressure = $0.5\rho V_m^2$
R_e	Earth's equatorial radius = 20,925,646 ft = 6378.13 km
R_p	Earth's polar radius = 20,855,486 ft = 6356.75 km
$\vec{r}$	vehicle's position vector
r	magnitude of $\vec{r}$
S	reference area = 116.2 ft^2
T	total thrust
T_0	total vacuum thrust
$(T_{aero.xb}, T_{aero.yb}, T_{aero.zb})$	body-axis components of aerodynamic torque
$(T_{rkt.xb}, T_{rkt.yb}, T_{rkt.zb})$	body-axis components of solid rocket torque
$(T_{rcs.xb}, T_{rcs.yb}, T_{rcs.zb})$	body-axis components of RCS torque
U	Earth's gravitational potential
(u, v, w)	body-axis components of $\vec{V}$
$\vec{V}$	vehicle's inertial velocity vector
$\vec{V}_{rel}$	vehicle's velocity vector relative to the Earth-fixed reference frame
$\vec{V}_w$	velocity vector of the wind
$\vec{V}_m$	air stream velocity vector
V_m	magnitude of the air stream velocity
$(V_{m.xb}, V_{m.yb}, V_{m.zb})$	body-axis components of vehicle's air stream velocity vector
(x, y, z)	inertial components of vehicle's position vector $\vec{r}$
X_a	aerodynamic reference point location in the structure frame = 275.6 ft
X_g	gimbal attach point location in the structural frame = 264.47 ft
X_{cp}	center of pressure (cp) location in the structure frame
$(\alpha,\ \beta)$	angle of attack and sideslip angle
δ_y	pitch gimbal angle (rotation about the body y-axis)
δ_z	yaw gimbal angle (rotation about the body z-axis)
μ	Earth's gravitational parameter = $1.407644176 \times 10^{16}$ ft^3/s^2
ϕ	Earth's geocentric latitude
Φ	Earth's geodetic latitude
$\boldsymbol{\Phi}$	flexible-mode influence matrix at gimbal attach point
$\boldsymbol{\Psi}$	flexible-mode influence matrix at instrument unit location
(ϕ, θ, ψ)	three Euler angles for a rotational sequence of $\boldsymbol{C}_1(\phi) \leftarrow \boldsymbol{C}_2(\theta) \leftarrow \boldsymbol{C}_3(\psi)$
ρ	atmospheric density (= 0.002377 slug/ft^2 at sea level)
$\boldsymbol{\eta}$	flexible-mode state vector
ζ	damping ratio of the flexible modes = 0.005
$\boldsymbol{\Omega} = diag(\omega_i)$	undamped natural frequency matrix of the flexible modes
$\vec{\omega}$	angular velocity vector of the vehicle
$\vec{\omega}_e = \omega_e \vec{K}$	angular velocity vector of the Earth where $\omega_e = 7.2921 \times 10^{-5}$ rad/s

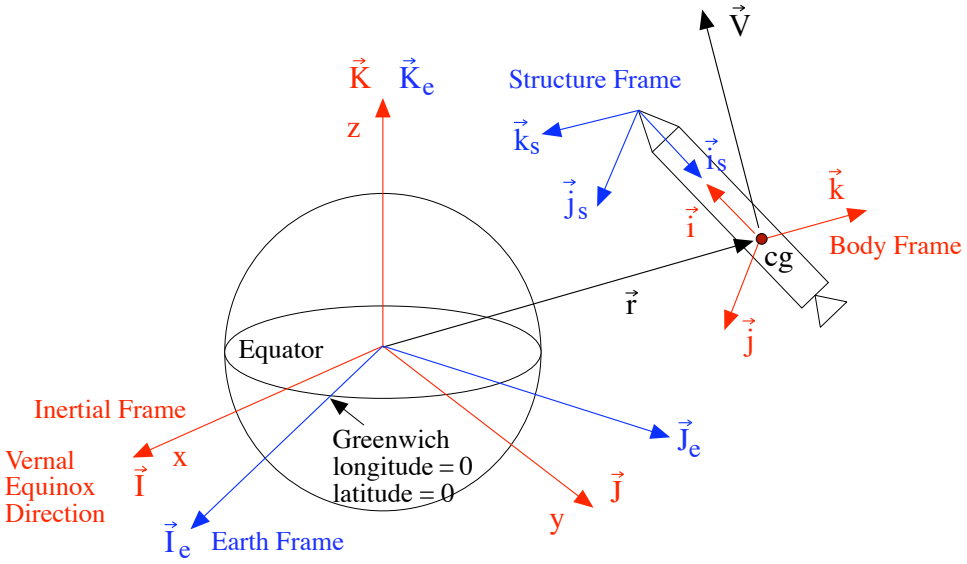

Figure 1. Illustration of the Earth-centered inertial reference frame with $\{\vec{I}, \vec{J}, \vec{K}\}$, the Earth-fixed reference frame with $\{\vec{I}_e, \vec{J}_e, \vec{K}_e\}$, the structure reference frame with $\{\vec{i}_s, \vec{j}_s, \vec{k}_s\}$, and the body-axis reference frame with $\{\vec{i}, \vec{j}, \vec{k}\}$.

I. Introduction

This paper describes the preliminary results of developing a complete set of coupled dynamic models and a Matlab-based simulation program for the Ares-I Crew Launch Vehicle (CLV), incorporating its propulsion, aerodynamics, guidance and control, and structural flexibility. The Ares-I CLV is a large, slender, and aerodynamically unstable vehicle. It is a two-stage rocket with a solid-propellant first stage derived from the Shuttle Reusable Solid Rocket Motor/Booster and an upper stage employing a J-2X engine derived from the Saturn J-2 engines.

NASA's Ares-I CLV reference model and the SAVANT Simulink-based program [1-3] were utilized to develop a Matlab-based simulation and linearization tool for an independent validation of the performance and stability of the ascent flight control system of the Ares-I CLV. Various dynamic models of launch vehicles available in the literature [4-8] were also utilized in this study.

Currently, the robust control design and stability analysis of the ascent flight control system of the Ares-I CLV are of practical interest [9-11]. In support of NASA's ascent flight control design efforts for the Ares-I CLV, we have also investigated the fundamental principles of flight control analysis and design for launch vehicles in a companion paper [12].

Nonlinear coupled dynamic simulation results of an ascent flight control system, which directly controls the inertial attitude-error quaternions and also employs non-minimum-phase filters, will be presented for a reference model of the Ares-I Crew Launch Vehicle. A linearized state-space model as well as a non-minimum-phase transfer function model of the Ares-I (which is of typical for flexible vehicles with non-collocated actuators and sensors) will also be presented for the ascent flight control design and analysis [12].

II. Reference Frames and Rotational Kinematics

Various reference frames and rotational kinematics, which are essential for describing the six-degrees-of-freedom dynamic model of launch vehicles, are briefly discussed in this section.

A. Earth-Centered Inertial Reference Frame

The Earth-centered inertial (ECI) frame with a set of basis vectors $\{\vec{I}, \vec{J}, \vec{K}\}$ has its origin at the Earth center as illustrated in Fig. 1. The x-axis points in the vernal equinox direction and the z-axis points in the direction of the north pole.

The position vector $\vec{r}$ of a launch vehicle is then described as

$$\vec{r} = x\vec{I} + y\vec{J} + z\vec{K} \tag{1}$$

The inertial velocity and the inertial acceleration of a launch vehicle become respectively

$$\vec{V} = \dot{x}\vec{I} + \dot{y}\vec{J} + \dot{z}\vec{K} \tag{2}$$

$$\dot{\vec{V}} = \ddot{x}\vec{I} + \ddot{y}\vec{J} + \ddot{z}\vec{K} \tag{3}$$

For example, if an inertial position vector of the Ares-I at liftoff from Kennedy Space Center (with longitude of 80.6-deg west and latitude of 28.4-deg north) is given by

$$\vec{r}(0) = x(0)\vec{I} + y(0)\vec{J} + z(0)\vec{K} = -8.7899E4\vec{I} - 1.8385E7\vec{J} + 9.9605E6\vec{K} \ \text{(ft)} \tag{4}$$

then, the inertial velocity vector of the vehicle at liftoff is obtained as

$$\vec{V}(0) = \dot{x}(0)\vec{I} + \dot{y}(0)\vec{J} + \dot{z}(0)\vec{K} = \vec{\omega}_e \times \vec{r}(0) = 1340.65\vec{I} - 6.41\vec{J} \ \text{(ft/sec)} \tag{5}$$

where $\vec{\omega}_e = \omega_e\vec{K}$ is the angular velocity vector of the Earth and $\omega_e = 7.2921 \times 10^{-5}$ rad/s which corresponds to 360 deg per a sidereal day of 23 h 56 min 4 s.

B. Earth-Fixed Equatorial Reference Frame

The geocentric equatorial rotating frame with a set of basis vectors $\{\vec{I}_e, \vec{J}_e, \vec{K}_e\}$, with its origin at the Earth center, is fixed to the Earth (Fig. 1). Its basis vector $\vec{I}_e$ is in the Greenwich meridian direction. This Earth-fixed frame rotates about $\vec{K} \equiv \vec{K}_e$ with an angular velocity ω_e.

C. Body-Axis Reference Frame

The body-axis reference frame with its basis vectors $\{\vec{i}, \vec{j}, \vec{k}\}$ is fixed to the vehicle's body as illustrated in Fig. 1. Its origin is located at the instant center of gravity. The $\vec{i}$-axis is along the vehicle's longitudinal axis. The $\vec{k}$-axis perpendicular to the $\vec{i}$-axis points downward while the $\vec{j}$-axis points rightward.

The inertial velocity vector $\vec{V}$ is then expressed as

$$\vec{V} = u\vec{i} + v\vec{j} + w\vec{k} \tag{6}$$

The angular velocity vector $\vec{\omega}$ of the launch vehicle is also expressed as

$$\vec{\omega} = p\vec{i} + q\vec{j} + r\vec{k} \tag{7}$$

The inertial acceleration vector is then described as

$$\dot{\vec{V}} = (\dot{u}\vec{i} + \dot{v}\vec{j} + \dot{w}\vec{k}) + \vec{\omega} \times \vec{V} \tag{8}$$

D. Structure Reference Frame

A structure reference frame with its basis vectors $\{\vec{i}_s, \vec{j}_s, \vec{k}_s\}$ and with its origin located at the top of vehicle is also employed in the SAVANT program. The locations of center of gravity, gimbal attach point, and aerodynamic reference point and other mass properties are defined using this structure frame. However, Euler's rotational equations of motion will be written in terms of the body-fixed frame with its origin at the center of gravity. Because $\vec{i}_s = -\vec{i}$, $\vec{j}_s = \vec{j}$, and $\vec{k}_s = -\vec{k}$, we have

$$\boldsymbol{C}^{B/S} = \begin{pmatrix} -1 & 0 & 0 \\ 0 & 1 & 0 \\ 0 & 0 & -1 \end{pmatrix} \tag{9}$$

where $\boldsymbol{C}^{B/S}$ is the direction cosine matrix of the frame B with respect to the frame S.

E. Euler Angles and Quaternions

The coordinate transformation to the body frame B from the inertial frame I is described by three Euler angles (ϕ, θ, ψ). For a rotational sequence of $\boldsymbol{C}_1(\phi) \leftarrow \boldsymbol{C}_2(\theta) \leftarrow \boldsymbol{C}_3(\psi)$, we have

$$\boldsymbol{C}^{B/I} = \begin{pmatrix} \cos\theta\cos\psi & \cos\theta\sin\psi & -\sin\theta \\ \sin\phi\sin\theta\cos\psi - \cos\phi\sin\psi & \sin\phi\sin\theta\sin\psi + \cos\phi\cos\psi & \sin\phi\cos\theta \\ \cos\phi\sin\theta\cos\psi + \sin\phi\sin\psi & \cos\phi\sin\theta\sin\psi - \sin\phi\cos\psi & \cos\phi\cos\theta \end{pmatrix} \tag{10}$$

which is the direction cosine matrix of the body frame B relative to the inertial frame I. However, the three Euler angles (ϕ, θ, ψ) do not actually represent the vehicle's roll, pitch, and yaw attitude angles to be used for attitude feedback control.

The rotational kinematic equation for three Euler angles (ϕ, θ, ψ) is given by

$$\begin{pmatrix} \dot{\phi} \\ \dot{\theta} \\ \dot{\psi} \end{pmatrix} = \frac{1}{\cos\theta} \begin{pmatrix} \cos\theta & \sin\phi\sin\theta & \cos\phi\sin\theta \\ 0 & \cos\phi\cos\theta & -\sin\phi\cos\theta \\ 0 & \sin\phi & \cos\phi \end{pmatrix} \begin{pmatrix} p \\ q \\ r \end{pmatrix} \tag{11}$$

The inherent singularity problem of Euler angles can be avoided by using quaternions. The rotational kinematic equation in terms of quaternions (q_1, q_2, q_3, q_4) is given by

$$\begin{pmatrix} \dot{q_1} \\ \dot{q_2} \\ \dot{q_3} \\ \dot{q_4} \end{pmatrix} = \frac{1}{2} \begin{pmatrix} 0 & r & -q & p \\ -r & 0 & p & q \\ q & -p & 0 & r \\ -p & -q & -r & 0 \end{pmatrix} \begin{pmatrix} q_1 \\ q_2 \\ q_3 \\ q_4 \end{pmatrix} \tag{12}$$

subject to the constraint: $q_1^2 + q_2^2 + q_3^2 + q_4^2 = 1$. The quaternions are related to the three Euler angles as follows:

$$\begin{aligned} q_1 &= \sin(\phi/2)\cos(\theta/2)\cos(\psi/2) - \cos(\phi/2)\sin(\theta/2)\sin(\psi/2) \\ q_2 &= \cos(\phi/2)\sin(\theta/2)\cos(\psi/2) + \sin(\phi/2)\cos(\theta/2)\sin(\psi/2) \\ q_3 &= \cos(\phi/2)\cos(\theta/2)\sin(\psi/2) - \sin(\phi/2)\sin(\theta/2)\cos(\psi/2) \\ q_4 &= \cos(\phi/2)\cos(\theta/2)\cos(\psi/2) + \sin(\phi/2)\sin(\theta/2)\sin(\psi/2) \end{aligned} \tag{13}$$

The coordinate transformation matrix to the body frame from the inertial frame in terms of quaternions is given by

$$\mathbf{C}^{B/I} = \begin{pmatrix} 1 - 2(q_2^2 + q_3^2) & 2(q_1q_2 + q_3q_4) & 2(q_1q_3 - q_2q_4) \\ 2(q_1q_2 - q_3q_4) & 1 - 2(q_1^2 + q_3^2) & 2(q_2q_3 + q_1q_4) \\ 2(q_1q_3 + q_2q_4) & 2(q_2q_3 - q_1q_4) & 1 - 2(q_1^2 + q_2^2) \end{pmatrix} \tag{14}$$

We also have

$$\mathbf{C}^{I/B} = [\mathbf{C}^{B/I}]^{-1} = [\mathbf{C}^{B/I}]^T = \begin{pmatrix} 1 - 2(q_2^2 + q_3^2) & 2(q_1q_2 - q_3q_4) & 2(q_1q_3 + q_2q_4) \\ 2(q_1q_2 + q_3q_4) & 1 - 2(q_1^2 + q_3^2) & 2(q_2q_3 - q_1q_4) \\ 2(q_1q_3 - q_2q_4) & 2(q_2q_3 + q_1q_4) & 1 - 2(q_1^2 + q_2^2) \end{pmatrix} \tag{15}$$

III. The 6-DOF Equations of Motion

The six-degrees-of-freedom (6-DOF) equations of motion of a launch vehicle consist of the translational and rotational equations. The translational equation of motion of the center of gravity of a launch vehicle is simply given by

$$m\dot{\vec{V}} = \vec{F} \tag{16}$$

where $\vec{F}$ is the total force acting on the vehicle. Using Eq. (3) and Eq. (8), we obtain the translational equation of motion of the form

$$\ddot{x}\vec{I} + \ddot{y}\vec{J} + \ddot{z}\vec{K} = \frac{\vec{F}}{m} \tag{17}$$

or

$$\dot{u}\vec{i} + \dot{v}\vec{j} + \dot{w}\vec{k} + \vec{\omega} \times \vec{V} = \frac{\vec{F}}{m} \tag{18}$$

The Euler's rotational equation of motion of a rigid vehicle is

$$\dot{\vec{H}} = \vec{T} \tag{19}$$

where $\vec{H}$ is the angular momentum vector and $\vec{T}$ is the total external torque about the center of gravity. The angular momentum vector is often expressed as

$$\vec{H} = \hat{I} \cdot \vec{\omega} \tag{20}$$

where $\vec{\omega} = p\vec{i} + q\vec{j} + r\vec{k}$ is the angular velocity vector and $\hat{I}$ is the vehicle's inertia dyadic about the center of gravity of the form [8]

$$\hat{I} = \begin{pmatrix} \vec{i} & \vec{j} & \vec{k} \end{pmatrix} \begin{pmatrix} I_{xx} & I_{xy} & I_{xz} \\ I_{xy} & I_{yy} & I_{yz} \\ I_{xz} & I_{yz} & I_{zz} \end{pmatrix} \begin{pmatrix} \vec{i} \\ \vec{j} \\ \vec{k} \end{pmatrix} \tag{21}$$

The rotational equation of motion is then given by

$$\hat{I} \cdot \dot{\vec{\omega}} + \vec{\omega} \times \hat{I} \cdot \vec{\omega} = \vec{T} \tag{22}$$

where $\dot{\vec{\omega}} = \dot{p}\vec{i} + \dot{q}\vec{j} + \dot{r}\vec{k}$ is the angular acceleration vector.

A. Aerodynamic Forces and Moments

Aerodynamic forces and moments depend on the vehicle's velocity relative to the surrounding air mass, called the air speed. It is assumed that the air mass is static relative to the Earth. That is, the entire air mass rotates with the Earth without slippage and shearing. The air stream velocity vector $\vec{V}_m$ is then described by

$$\vec{V}_m = \vec{V}_{rel} - \vec{V}_w = \vec{V} - \vec{\omega}_e \times \vec{r} - \vec{V}_w \tag{23}$$

where $\vec{V}_{rel}$ is the vehicle's velocity vector relative to the Earth-fixed reference frame, $\vec{V}_w$ is the local disturbance wind velocity, $\vec{V}$ is the inertial velocity of the vehicle, and $\vec{\omega}_e$ is the Earth's rotational angular velocity vector, and $\vec{r}$ is the vehicle's position vector from the Earth center.

The matrix form of Eq. (23) in the body frame is

$$\begin{pmatrix} V_{m.xb} \\ V_{m.yb} \\ V_{m.zb} \end{pmatrix} = \begin{pmatrix} u \\ v \\ w \end{pmatrix} - \mathbf{C}^{B/I} \begin{pmatrix} 0 & -\omega_e & 0 \\ \omega_e & 0 & 0 \\ 0 & 0 & 0 \end{pmatrix} \begin{pmatrix} x \\ y \\ z \end{pmatrix} - \begin{pmatrix} V_{w.xb} \\ V_{w.yb} \\ V_{w.zb} \end{pmatrix} \tag{24}$$

where $(V_{m.xb}, V_{m.yb}, V_{m.zb})$ are the body-axis components of the vehicle's air stream velocity vector. Note that $\vec{r} = x\vec{I} + y\vec{J} + z\vec{K}$ and $\vec{\omega}_e = \omega_e\vec{K}$.

The aerodynamic forces are expressed in the body-axis frame as

$$\begin{aligned} D &= C_A QS - F_{base} \\ C &= C_{Y\beta}\beta QS \\ N &= (C_{N0} + C_{N\alpha}\alpha)QS \end{aligned} \tag{25}$$

where the base force F_{base} is a function of the altitude, the aerodynamic force coefficients are functions of Mach number, and

$$M = \frac{V_m}{a} = \text{Mach number} \tag{26}$$

$$Q = \frac{1}{2}\rho V_m^2 = \text{dynamic pressure} \tag{27}$$

$$\alpha = \arctan\left\{\frac{V_{m.zb}}{V_{m.xb}}\right\} = \text{angle of attack} \tag{28}$$

$$\beta = \arcsin\left\{\frac{V_{m.yb}}{V_m}\right\} = \text{sideslip angle} \tag{29}$$

The speed of sound a and the air density ρ are functions of the altitude h.

Furthermore, we have

$$\begin{aligned} F_{aero.xb} &= -D \\ F_{aero.yb} &= C \\ F_{aero.zb} &= -N \end{aligned} \tag{30}$$

The aerodynamic moments about the center of gravity are also expressed in the body-axis frame as

$$\begin{pmatrix} T_{aero.xb} \\ T_{aero.yb} \\ T_{aero.zb} \end{pmatrix} = \begin{pmatrix} 0 & c_z & -c_y \\ -c_z & 0 & -X_a + c_x \\ c_y & X_a - c_x & 0 \end{pmatrix} \begin{pmatrix} F_{aero.xb} \\ F_{aero.yb} \\ F_{aero.zb} \end{pmatrix} + \begin{pmatrix} C_{Mr\beta} QSb \\ (C_{Mp0} + C_{Mp\alpha}\alpha) QSb \\ C_{my\beta}\beta QSb \end{pmatrix} \tag{31}$$

where $X_a = 275.6$ ft is the aerodynamic reference point in the structure frame, (c_x, c_y, c_z) is the center of gravity location in the structure reference frame with its origin at the top of vehicle. At $t = 0$, we have $(c_x, c_y, c_z) = (220.31, 0.02, 0.01)$ ft. The aerodynamic moment coefficients are functions of Mach number.

B. Gravity Model

The J4 gravity model used in the SAVANT program is described as

$$C_1 = -1 + \frac{R_e^2}{r^2}\left[3J_2\left(\frac{3}{2}\sin^2\phi - \frac{1}{2}\right) + 4J_3\frac{R_e}{r}\left(\frac{5}{2}\sin^3\phi - \frac{3}{2}\sin\phi\right) + 5J_4\frac{R_e^2}{r^2}\left(\frac{35}{8}\sin^4\phi - \frac{15}{4}\sin^2\phi + \frac{3}{8}\right)\right] \tag{32}$$

where ϕ is the Earth's geocentric latitude.

$$C_2 = J_2(3\sin\phi) + \frac{R_e}{r}J_3\left(\frac{15}{2}\sin^2\phi - \frac{3}{2}\right) + \frac{R_e^2}{r^2}J_4\left(\frac{35}{2}\sin^3\phi - \frac{15}{2}\sin\phi\right) \tag{33}$$

The inertial components of the gravitational acceleration are

$$\begin{pmatrix} g_x \\ g_y \\ g_z \end{pmatrix} = \frac{\mu}{r^2}\left[C_1\begin{pmatrix} x/r \\ y/r \\ z/r \end{pmatrix} - C_2\begin{pmatrix} 0 & -z/r & y/r \\ z/r & 0 & -x/r \\ -y/r & x/r & 0 \end{pmatrix}\begin{pmatrix} -y/r \\ x/r \\ 0 \end{pmatrix}\right] \tag{34}$$

The mathematical models used in the SAVANT program for computing the vehicle's altitude h are summarized as

$$f = \frac{R_e - R_p}{R_e} = \frac{1}{298.257} \tag{35}$$

$$\tan\Phi = \frac{\tan\phi}{(1-f)^2} \tag{36}$$

$$A = \left(\frac{\cos\Phi}{R_e}\right)^2 + \left(\frac{\sin\Phi}{R_p}\right)^2 \tag{37}$$

$$B = -\frac{\sqrt{x^2+y^2}\cos\Phi}{R_e^2} - \frac{z\sin\Phi}{R_p^2} \tag{38}$$

$$C = \left(\frac{z}{R_p}\right)^2 + \frac{x^2+y^2}{R_p^2} - 1 \tag{39}$$

$$h = -\frac{B}{A} - \sqrt{\left(\frac{B}{A}\right)^2 - \frac{C}{A}} \tag{40}$$

where f is the Earth's flatness parameter, ϕ is the geocentric latitude, and Φ is the geodetic latitude (which is commonly employed on geographical maps).

C. Rocket Propulsion Model

The rocket thrust is simply modeled as

$$T = T_0 + (p_e - p_0)A_e \tag{41}$$

where T is the total thrust force, $T_0 = |\dot{m}|V_e$ the total vacuum thrust, p_e the nozzle exit pressure, p_0 the local atmospheric pressure (a function of the altitude), $\dot{m}$ the propellant mass flow rate, V_e the exit velocity, and A_e the nozzle exit area (= 122.137 ft^2).

The body-axis components of the thrust force are

$$\begin{pmatrix} F_{rkt.xb} \\ F_{rkt.yb} \\ F_{rkt.zb} \end{pmatrix} = \begin{pmatrix} T \\ -T\delta_z \\ T\delta_y \end{pmatrix} \tag{42}$$

where δ_y and δ_z are the pitch and yaw gimbal deflection angles, respectively. Gimbal deflection angles are assumed to be small (with $\delta_{max} = \pm 10$ deg).

The body-axis components of the rocket thrust-generated torque are

$$\begin{pmatrix} T_{rkt.xb} \\ T_{rkt.yb} \\ T_{rkt.zb} \end{pmatrix} = \begin{pmatrix} 0 & c_z & -c_y \\ -c_z & 0 & -X_g + c_x \\ c_y & X_g - c_z & 0 \end{pmatrix} \begin{pmatrix} F_{rkt.xb} \\ F_{rkt.yb} \\ F_{rkt.zb} \end{pmatrix} \tag{43}$$

where $X_g = 296$ ft is the gimbal attach point location in the structure frame.

The body-axis components of the roll control torque from the reaction control system (RCS) are

$$\begin{pmatrix} T_{rcs.xb} \\ T_{rcs.yb} \\ T_{rcs.zb} \end{pmatrix} = \begin{pmatrix} T_{rcs} \\ 0 \\ 0 \end{pmatrix} \tag{44}$$

D. Guidance and Control

The commanded quaternions $(q_{1c}, q_{2c}, q_{3c}, q_{4c})$ computed by the guidance system is used to generate the attitude-error quaternions $(q_{1e}, q_{2e}, q_{3e}, q_{4e})$ as follows [8]:

$$\begin{pmatrix} q_{1e} \\ q_{2e} \\ q_{3e} \\ q_{4e} \end{pmatrix} = \begin{pmatrix} q_{4c} & q_{3c} & -q_{2c} & -q_{1c} \\ -q_{3c} & q_{4c} & q_{1c} & -q_{2c} \\ q_{2c} & -q_{1c} & q_{4c} & -q_{3c} \\ q_{1c} & q_{2c} & q_{3c} & q_{4c} \end{pmatrix} \begin{pmatrix} q_1 \\ q_2 \\ q_3 \\ q_4 \end{pmatrix} \tag{45}$$

where the attitude quaternions (q_1, q_2, q_3, q_4) are computed by numerically integrating the following kinematic differential equations:

$$\begin{pmatrix} \dot{q_1} \\ \dot{q_2} \\ \dot{q_3} \\ \dot{q_4} \end{pmatrix} = \frac{1}{2} \begin{pmatrix} 0 & r & -q & p \\ -r & 0 & p & q \\ q & -p & 0 & r \\ -p & -q & -r & 0 \end{pmatrix} \begin{pmatrix} q_1 \\ q_2 \\ q_3 \\ q_4 \end{pmatrix} \tag{46}$$

The simplified control laws of the ascent flight control system are then described as

$$T_{rcs} = -K_{px}(2q_{1e}) - K_{dx}p \tag{47}$$

$$\delta_y = -K_{py}(2q_{2e}) - K_{iy}\int (2q_{2e})dt - K_{dy}q \tag{48}$$

$$\delta_z = -K_{pz}(2q_{3e}) - K_{dz}r \tag{49}$$

An integral control is added to the pitch control channel. The terms $(2q_{1e}, 2q_{2e}, 2q_{3e})$ are the roll, pitch, and yaw attitude errors, respectively. This quaternion-error feedback control is in general applicable for an arbitrarily large angular motion of vehicles [8]. Feedback of Euler-angle errors $(\phi - \phi_c, \theta - \theta_c, \psi - \psi_c)$ is not applicable here because the Euler angles employed in this paper (also used in the SAVANT program) are defined with respect to the Earth-centered inertial reference frame, not with respect to the so-called pitch plane or a navigation reference frame of launch vehicles [4-8, 11].

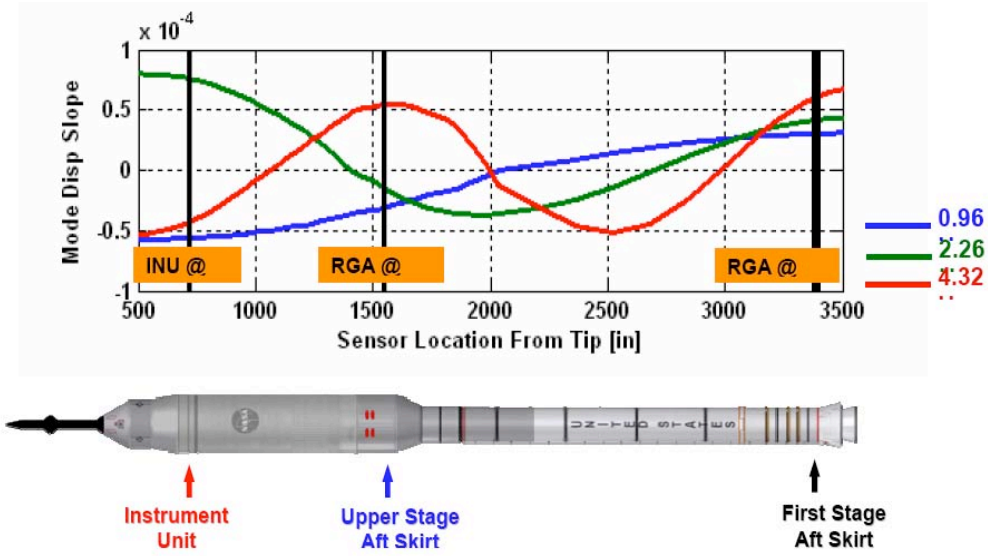

Figure 2. Flexible mode shapes and sensor locations of the Ares-I Crew Launch Vehicle [1]. Currently, rate-gyro blending is not considered for the Ares-I.

E. Flexible-Body Modes

A flexible-body model of launch vehicles is often expressed as

$$\ddot{\boldsymbol{\eta}} + 2\zeta\boldsymbol{\Omega}\dot{\boldsymbol{\eta}} + \boldsymbol{\Omega}^2\boldsymbol{\eta} = \boldsymbol{\Phi}^T \boldsymbol{F}_{rkt} \tag{50}$$

where $\boldsymbol{F}_{rkt} = (F_{rkt.xb}, F_{rkt.yb}, F_{rkt.zb})^T$ and $\boldsymbol{\Phi}$ is the flex-mode influence matrix at the gimbal attach point.

Sensor measurements including the effects of the flexible bending modes are modeled as

$$\boldsymbol{e}_{attitude} = \begin{pmatrix} 2q_{1e} \\ 2q_{2e} \\ 2q_{3e} \end{pmatrix} + \boldsymbol{\Psi}\boldsymbol{\eta} \tag{51}$$

$$\boldsymbol{e}_{rate} = \begin{pmatrix} p \\ q \\ r \end{pmatrix} + \boldsymbol{\Psi}\dot{\boldsymbol{\eta}} \tag{52}$$

where $\boldsymbol{\Psi}$ is the flex-mode influence matrix at the instrument unit location (Fig. 2).

F. A Summary of the 6-DOF Equations of Motion

Total force expressed in the body frame:

$$\begin{pmatrix} F_{total.xb} \\ F_{total.yb} \\ F_{total.zb} \end{pmatrix} = \begin{pmatrix} F_{aero.xb} \\ F_{aero.yb} \\ F_{aero.zb} \end{pmatrix} + \begin{pmatrix} F_{rkt.xb} \\ F_{rkt.yb} \\ F_{rkt.zb} \end{pmatrix} + \begin{pmatrix} F_{rcs.xb} \\ F_{rcs.yb} \\ F_{rcs.zb} \end{pmatrix} \tag{53}$$

Total force expressed in the inertial frame:

$$\begin{pmatrix} F_{total.xi} \\ F_{total.yi} \\ F_{total.zi} \end{pmatrix} = \boldsymbol{C}^{I/B} \begin{pmatrix} F_{total.xb} \\ F_{total.yb} \\ F_{total.zb} \end{pmatrix} \tag{54}$$

Table 1. Initial conditions at liftoff

State variables	Initial values	Units
$\dot{x}$	1340.65	ft/s
$\dot{y}$	-6.41	ft/s
$\dot{z}$	0	ft/s
x	-8.7899×10^4	ft
y	-1.8385×10^7	ft
z	9.9605×10^6	ft
p	3.4916×10^{-5}	rad/s
q	6.4018×10^{-5}	rad/s
r	0	rad/s
q_1	0.3594	
q_2	-0.6089	
q_3	-0.3625	
q_4	0.6072	

Translational equation in the inertial frame:

$$\begin{pmatrix} \ddot{x} \\ \ddot{y} \\ \ddot{z} \end{pmatrix} = \frac{1}{m} \begin{pmatrix} F_{total.xi} \\ F_{total.yi} \\ F_{total.zi} \end{pmatrix} + \begin{pmatrix} g_x \\ g_y \\ g_z \end{pmatrix} \tag{55}$$

Rotational equation in the body frame:

$$\begin{aligned} \begin{pmatrix} I_{xx} & I_{xy} & I_{xz} \\ I_{xy} & I_{yy} & I_{yz} \\ I_{xz} & I_{yz} & I_{zz} \end{pmatrix} \begin{pmatrix} \dot{p} \\ \dot{q} \\ \dot{r} \end{pmatrix} = &- \begin{pmatrix} 0 & -r & q \\ r & 0 & -p \\ -q & p & 0 \end{pmatrix} \begin{pmatrix} I_{xx} & I_{xy} & I_{xz} \\ I_{xy} & I_{yy} & I_{yz} \\ I_{xz} & I_{yz} & I_{zz} \end{pmatrix} \begin{pmatrix} p \\ q \\ r \end{pmatrix} \\ &+ \begin{pmatrix} T_{aero.xb} \\ T_{aero.yb} \\ T_{aero.zb} \end{pmatrix} + \begin{pmatrix} T_{rkt.xb} \\ T_{rkt.yb} \\ T_{rkt.zb} \end{pmatrix} + \begin{pmatrix} T_{rcs.xb} \\ T_{rcs.yb} \\ T_{rcs.zb} \end{pmatrix} \end{aligned} \tag{56}$$

$$\begin{pmatrix} \dot{q_1} \\ \dot{q_2} \\ \dot{q_3} \\ \dot{q_4} \end{pmatrix} = \frac{1}{2} \begin{pmatrix} 0 & r & -q & p \\ -r & 0 & p & q \\ q & -p & 0 & r \\ -p & -q & -r & 0 \end{pmatrix} \begin{pmatrix} q_1 \\ q_2 \\ q_3 \\ q_4 \end{pmatrix} \tag{57}$$

IV. Simulation Results of the Ares-I Crew Launch Vehicle

A set of initial conditions for the Ares-I is provided in Table 1. The corresponding initial conditions for Euler angles are: (ϕ, θ, ψ) = (90, -28.61, -90.28) deg. The inertia matrix about the body frame with its origin at the center of gravity at $t = 0$ is

$$\begin{pmatrix} I_{xx} & I_{xy} & I_{xz} \\ I_{xy} & I_{yy} & I_{yz} \\ I_{xz} & I_{yz} & I_{zz} \end{pmatrix} = \begin{pmatrix} 1.2634E6 & -1.5925E3 & 5.5250E4 \\ -1.5925E3 & 2.8797E8 & -1.5263E3 \\ 5.5250E4 & -1.5263E3 & 2.8798E8 \end{pmatrix} \text{ slug-ft}^2 \tag{58}$$

Flexible-body mode shape matrices (with 6 flexible modes) are

$$\mathbf{\Phi} = \begin{pmatrix} 0.000000272367963 & 0.000000174392026 & -0.000000347086527 \\ -0.000364943105155 & 0.006281028219530 & 0.000491932740239 \\ 0.006281175443849 & 0.000364891432306 & -0.006260333099131 \\ -0.000000266173427 & 0.000000329288262 & -0.000000369058169 \\ -0.006259406451949 & -0.000542750533582 & -0.007673360355205 \\ -0.000491798506301 & 0.007676195145027 & -0.000542218216634 \end{pmatrix} \tag{59}$$

$$\mathbf{\Psi} = \begin{pmatrix} 0.002287263504447 & -0.003936428406260 & -0.002315093057592 \\ -0.193164818571118 & -0.011222878633268 & -0.253963647069578 \\ -0.011222390194941 & 0.193169876159476 & -0.019955470041040 \\ 0.003866041325542 & 0.002898204936058 & 0.005033045198158 \\ -0.019956097043432 & -0.130518411476224 & 0.009224310239736 \\ 0.253971718426341 & -0.009226496087855 & -0.130493158175449 \end{pmatrix} \times 10^{-3} \tag{60}$$

The first three bending mode frequencies are: 6 rad/s, 14 rad/s, and 27 rad/s. The damping ratio is assumed as $\zeta = 0.005$.

The simulation results of a test case for a Matlab-based simulation program are shown in Fig. 3-19. These results are identical to those obtained using the SAVANT program for the same test case. However, these simulation results were for a preliminary reference model of the Ares-I available to the public, not for the most recent model of the Ares-I with properly updated, ascent flight guidance and control algorithms. Our study purpose was to develop a Matlab-based simulation tool for an independent validation of the performance and stability of NASA's ascent flight control system design for the Ares-I.

The center of pressure (cp) location shown in Fig. 11 was computed as

$$X_{cp} = X_a - \frac{(C_{Mp0} + C_{Mp\alpha}\alpha)b}{C_{N0} + C_{N\alpha}\alpha} \tag{61}$$

where X_{cp} is the distance to the cp location from the top of vehicle and X_a is the distance to the aerodynamic reference point from the top of vehicle (i.e., the origin of the structure reference frame).

V. Linear Rigid-Body Model

A. Nonlinear 6-DOF Equations

Translational equations in the body frame:

$$\begin{pmatrix} \dot{u} \\ \dot{v} \\ \dot{w} \end{pmatrix} = -\begin{pmatrix} 0 & -r & q \\ r & 0 & -p \\ -q & p & 0 \end{pmatrix}\begin{pmatrix} u \\ v \\ w \end{pmatrix} + \boldsymbol{C}^{B/I}\begin{pmatrix} g_x \\ g_y \\ g_z \end{pmatrix} + \frac{1}{m}\begin{pmatrix} F_{aero.xb} \\ F_{aero.yb} \\ F_{aero.zb} \end{pmatrix} + \frac{1}{m}\begin{pmatrix} T \\ -T\delta_z \\ T\delta_y \end{pmatrix} \tag{62}$$

where

$$\mathbf{C}^{B/I} = \begin{pmatrix} 1-2(q_2^2+q_3^2) & 2(q_1q_2+q_3q_4) & 2(q_1q_3-q_2q_4) \\ 2(q_1q_2-q_3q_4) & 1-2(q_1^2+q_3^2) & 2(q_2q_3+q_1q_4) \\ 2(q_1q_3+q_2q_4) & 2(q_2q_3-q_1q_4) & 1-2(q_1^2+q_2^2) \end{pmatrix} \tag{63}$$

Rotational equation in the body frame:

$$\begin{pmatrix} I_{xx} & I_{xy} & I_{xz} \\ I_{xy} & I_{yy} & I_{yz} \\ I_{xz} & I_{yz} & I_{zz} \end{pmatrix}\begin{pmatrix} \dot{p} \\ \dot{q} \\ \dot{r} \end{pmatrix} = -\begin{pmatrix} 0 & -r & q \\ r & 0 & -p \\ -q & p & 0 \end{pmatrix}\begin{pmatrix} I_{xx} & I_{xy} & I_{xz} \\ I_{xy} & I_{yy} & I_{yz} \\ I_{xz} & I_{yz} & I_{zz} \end{pmatrix}\begin{pmatrix} p \\ q \\ r \end{pmatrix} + \begin{pmatrix} T_{aero.xb} \\ T_{aero.yb} \\ T_{aero.zb} \end{pmatrix} + \begin{pmatrix} T_{rkt.xb} \\ T_{rkt.yb} \\ T_{rkt.zb} \end{pmatrix} + \begin{pmatrix} T_{rcs.xb} \\ T_{rcs.yb} \\ T_{rcs.zb} \end{pmatrix} \tag{64}$$

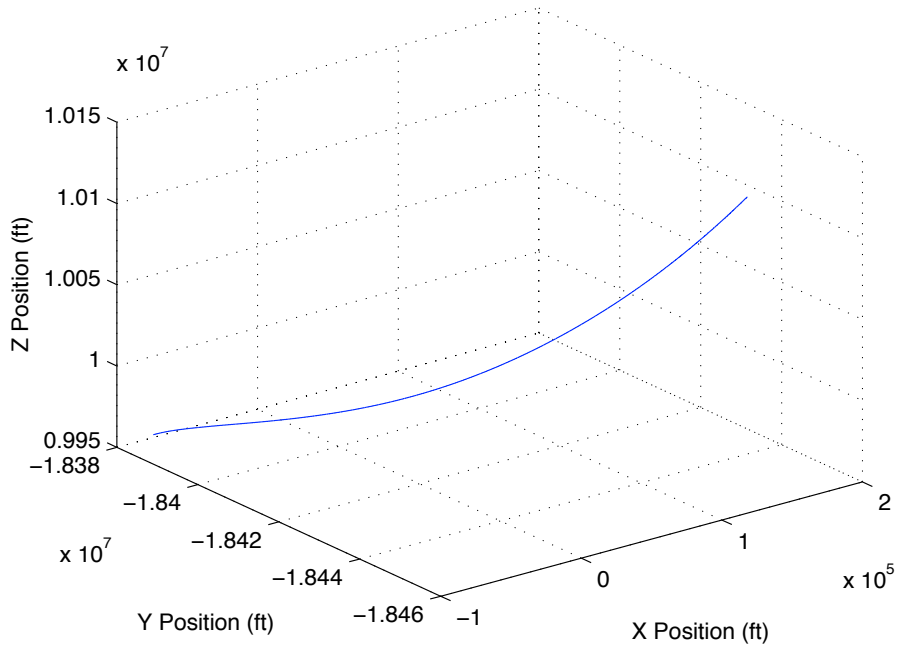

Figure 3. Vehicle's position (x, y, z) in the Earth-centered inertial reference frame.

B. Linearization Results

$$\Delta\dot{u} = r_0\Delta v - q_0\Delta w - w_0\Delta q + v_0\Delta r + (2g_yq_{2c} + 2g_zq_{3c})\Delta q_1 + (-4g_xq_{2c} + 2g_yq_{1c} - 2g_zq_{4c})\Delta q_2 \\ +(-4g_xq_{3c} + 2g_yq_{4c} + 2g_zq_{1c})\Delta q_3 + (2g_yq_{3c} - 2g_zq_{2c})\Delta q_4 + \tfrac{1}{m}\Delta F_{aero.xb} \tag{65}$$

$$\Delta\dot{v} = -r_0\Delta u + p_0\Delta w + w_0\Delta p - u_0\Delta r + (2g_xq_{2c} - 4g_yq_{1c} + 2g_zq_{4c})\Delta q_1 + (2g_xq_{1c} + 2g_zq_{3c})\Delta q_2 \\ +(-2g_xq_{4c} - 4g_yq_{3c} + 2g_zq_{2c})\Delta q_3 + (-2g_xq_{3c} + 2g_zq_{1c})\Delta q_4 + \tfrac{1}{m}\Delta F_{aero.yb} + (-\tfrac{T}{m})\Delta\delta_z \tag{66}$$

$$\Delta\dot{w} = q_0\Delta u - p_0\Delta v - v_0\Delta p + u_0\Delta q + (2g_xq_{3c} - 2g_yq_{4c} - 4g_zq_{1c})\Delta q_1 + (2g_xq_{4c} + 2g_yq_{3c} - 4g_zq_{2c})\Delta q_2 \\ +(2g_xq_{1c} + 2g_yq_{2c})\Delta q_3 + (2g_xq_{2c} - 2g_yq_{1c})\Delta q_4 + \tfrac{1}{m}\Delta F_{aero.zb} + (\tfrac{T}{m})\Delta\delta_y \tag{67}$$

$$\begin{pmatrix} I_{xx} & 0 & 0 \\ 0 & I_{yy} & 0 \\ 0 & 0 & I_{zz} \end{pmatrix} \begin{pmatrix} \Delta\dot{p} \\ \Delta\dot{q} \\ \Delta\dot{r} \end{pmatrix} = \begin{pmatrix} b_1 \\ b_2 \\ b_3 \end{pmatrix} \tag{68}$$

where the relatively small products of inertia are ignored, and

$$b_1 = [r_0I_{yy} - I_{zz}r_0]\Delta q + [I_{yy}q_0 - q_0I_{zz}]\Delta r + \Delta T_{aero.xb} + (-c_yT)\Delta\delta_y + (-c_zT)\Delta\delta_z + \Delta T_{rcs} \tag{69}$$

$$b_2 = [-r_0I_{yy} + I_{zz}r_0)]\Delta p + [-(I_{xx}p_0 + p_0I_{zz}]\Delta r + \Delta T_{aero.yb} + (c_x - X_g)T\Delta\delta_y \tag{70}$$

$$b_3 = [q_0I_{xx} - +I_{yy}q_0+]\Delta p + [(I_{xx}p_0 - p_0I_{yy}]\Delta q + \Delta T_{aero.zb} + (X_g - c_x)(-T)\Delta\delta_z \tag{71}$$

$$\Delta\dot{q_1} = \frac{1}{2}(q_{4c}\Delta p - q_{3c}\Delta q + q_{2c}\Delta r + r_0\Delta q_2 - q_0\Delta q_3 + p_0\Delta q_4) \tag{72}$$

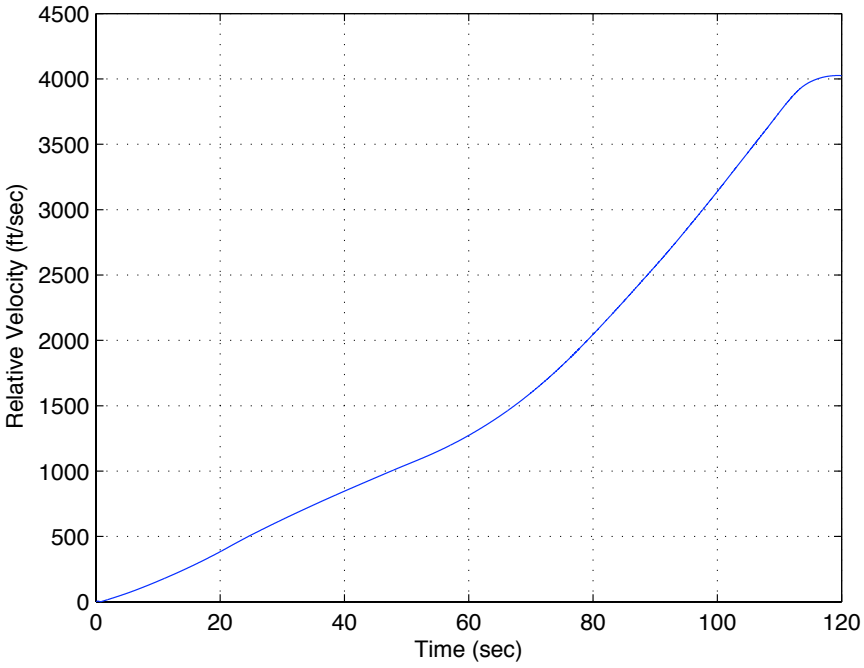

Figure 4. Relative velocity V_{rel} with respect to the Earth-fixed reference frame.

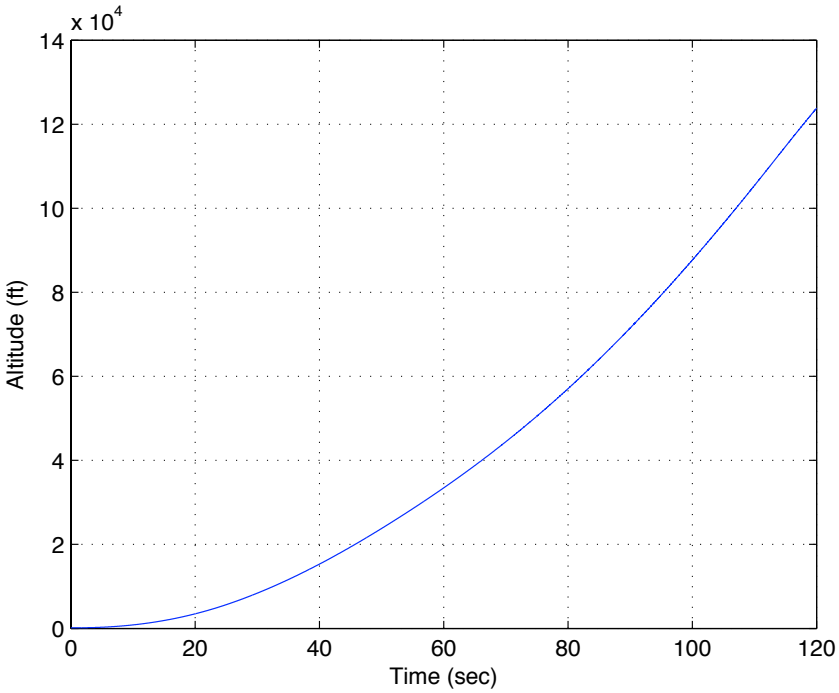

Figure 5. Altitude h.

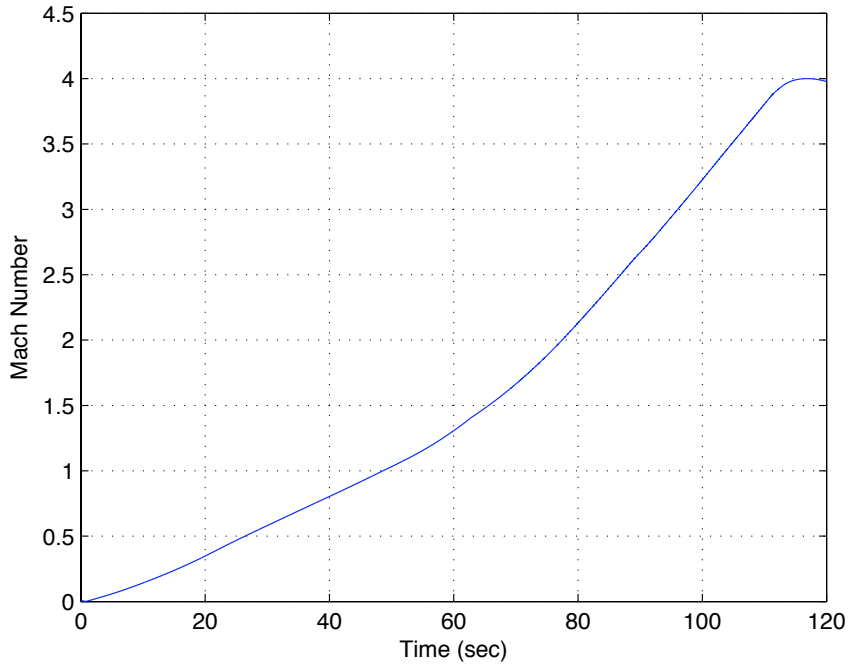

Figure 6. Mach number M.

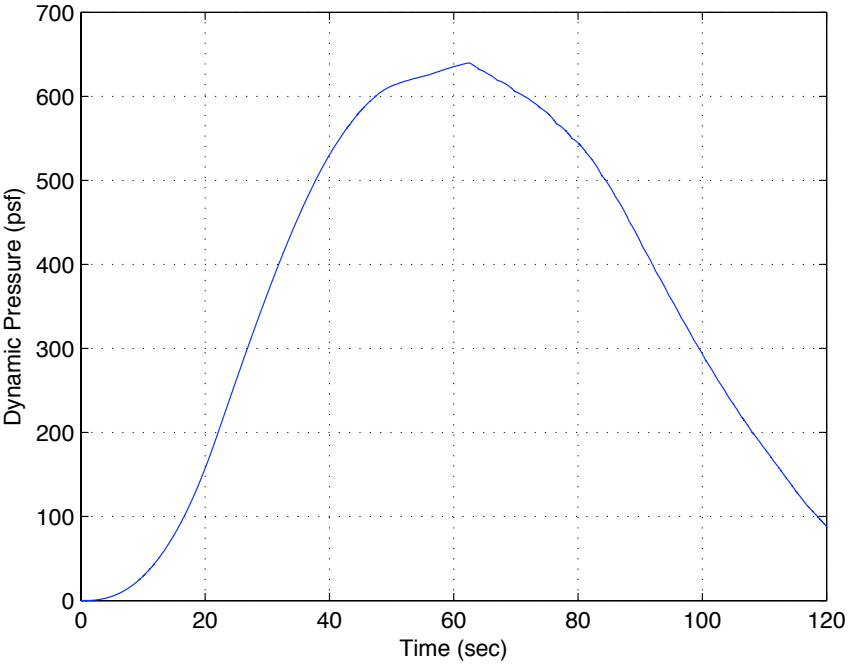

Figure 7. Dynamic pressure Q in units of lb/ft^2.

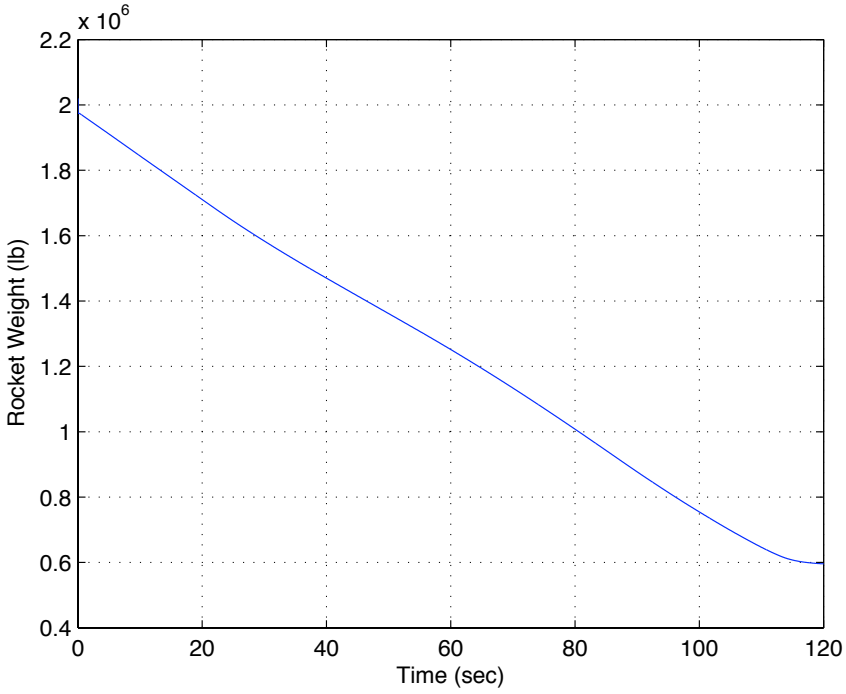

Figure 8. Vehicle's total weight mg.

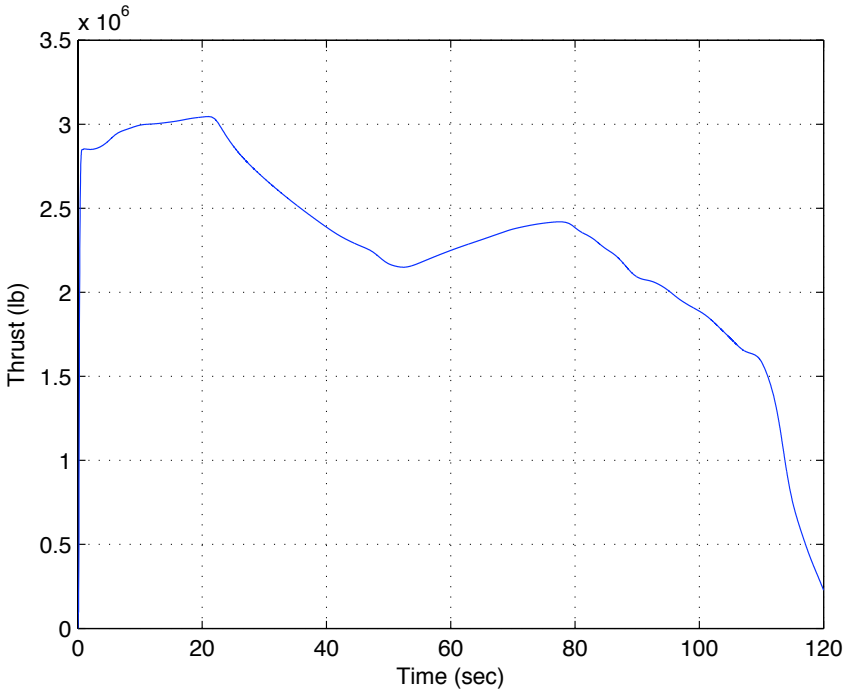

Figure 9. Total thrust T.

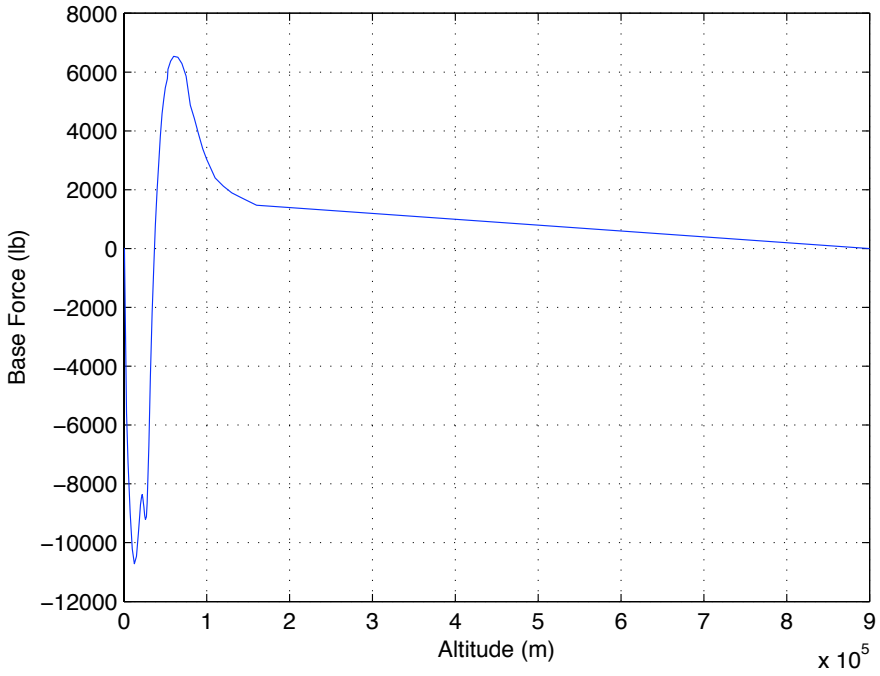

Figure 10. Base force F_{base} as a function of altitude in units of meters.

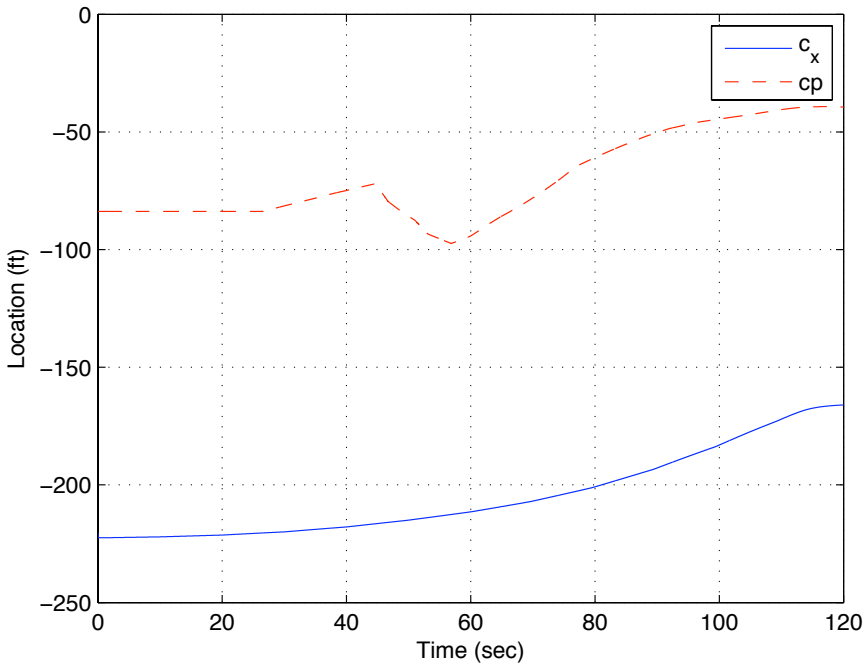

Figure 11. Locations of the center of pressure (cp) and the center of gravity (cg) from the top of vehicle.

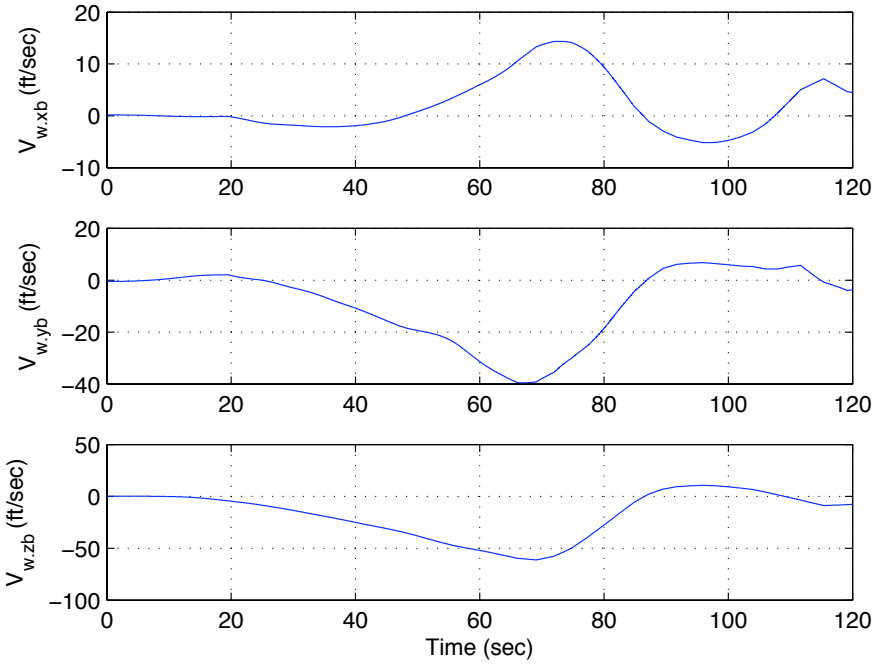

Figure 12. Disturbance wind velocity components in the body frame.

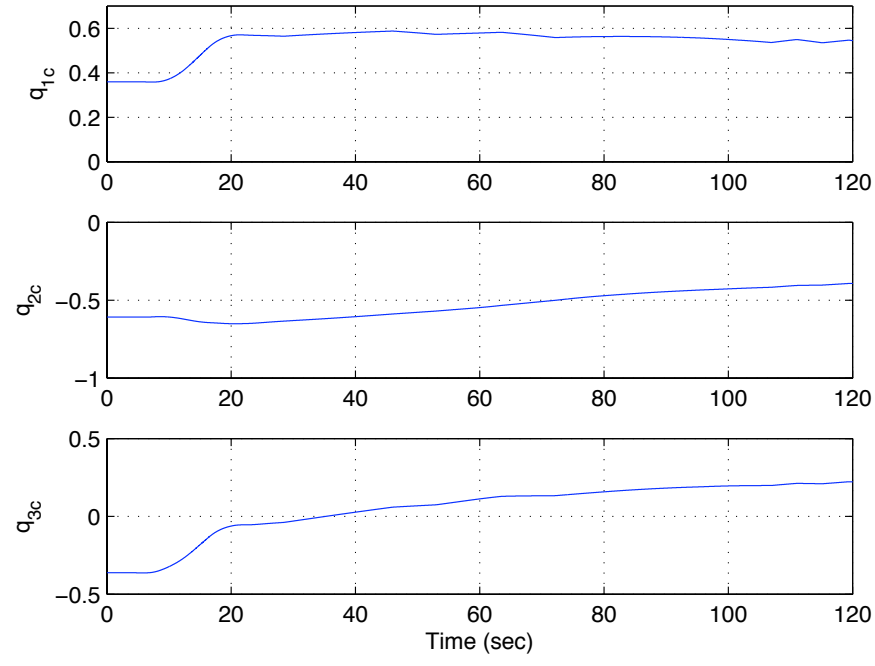

Figure 13. Commanded quaternions (q_{4c} not shown).

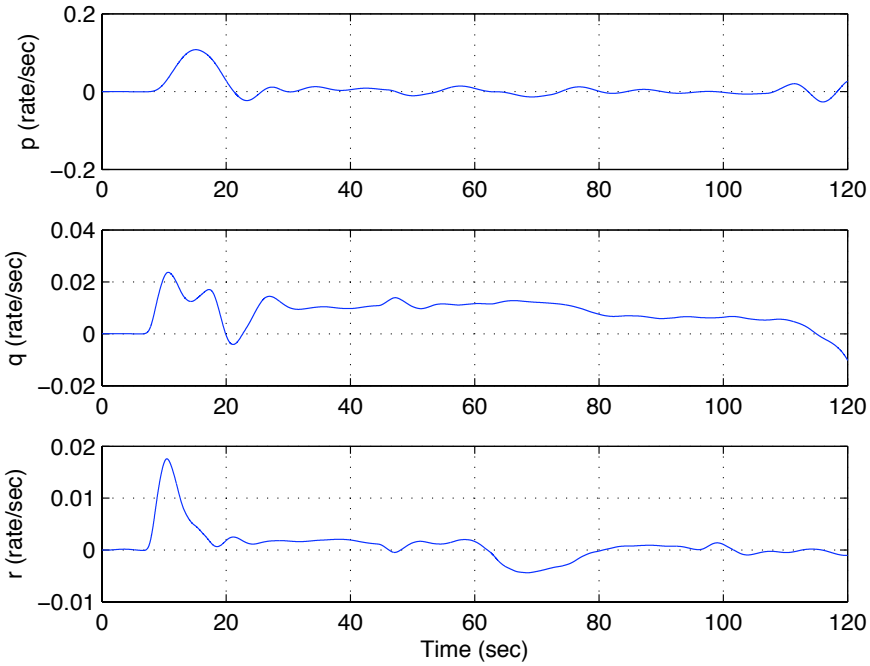

Figure 14. Body angular rates (p, q, r).

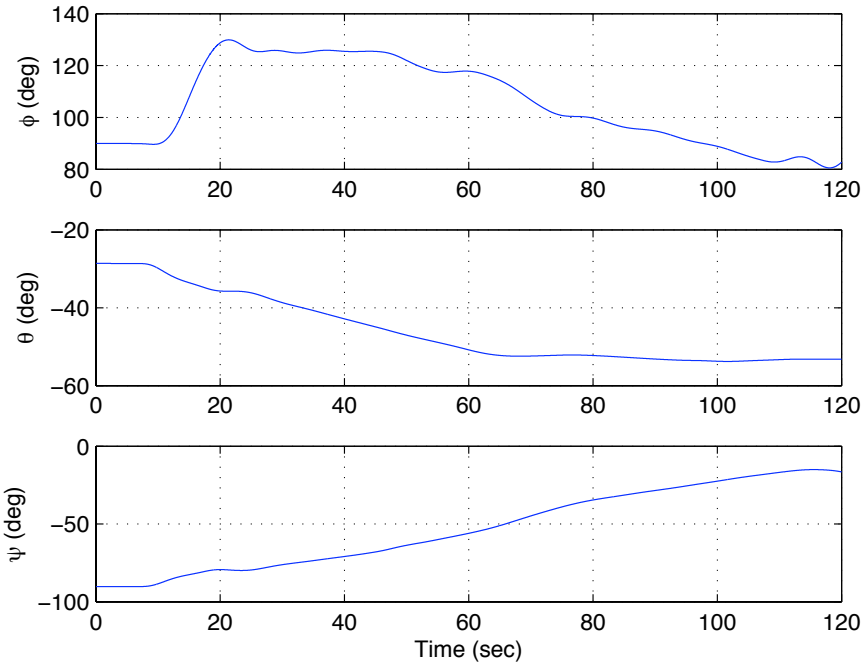

Figure 15. Euler angles (ϕ, θ, ψ). These Euler angles (ϕ, θ, ψ) do not actually represent the vehicle's roll, pitch, and yaw attitude angles for attitude feedback control.

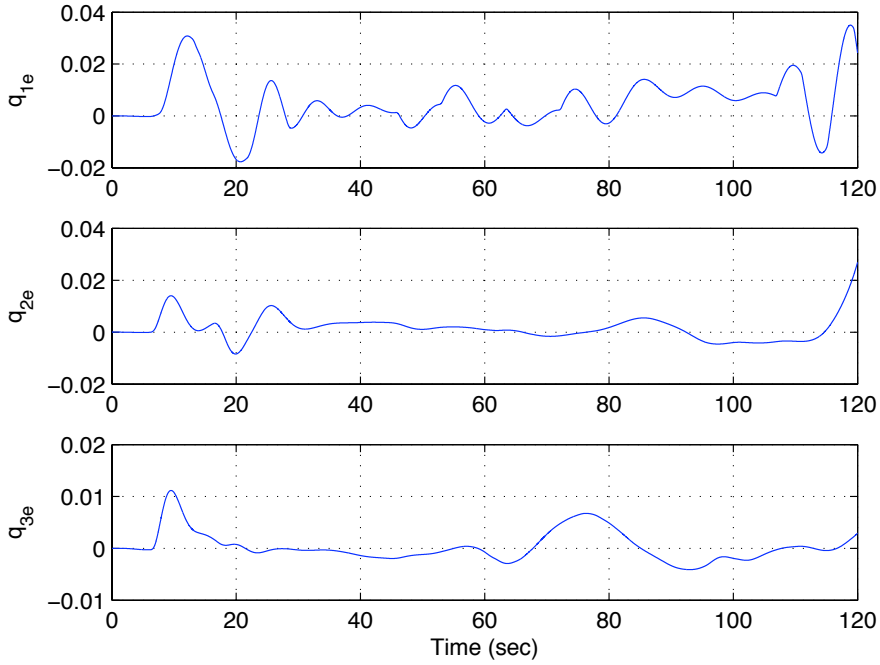

Figure 16. Attitude-error quaternions (q_{4e} not shown).

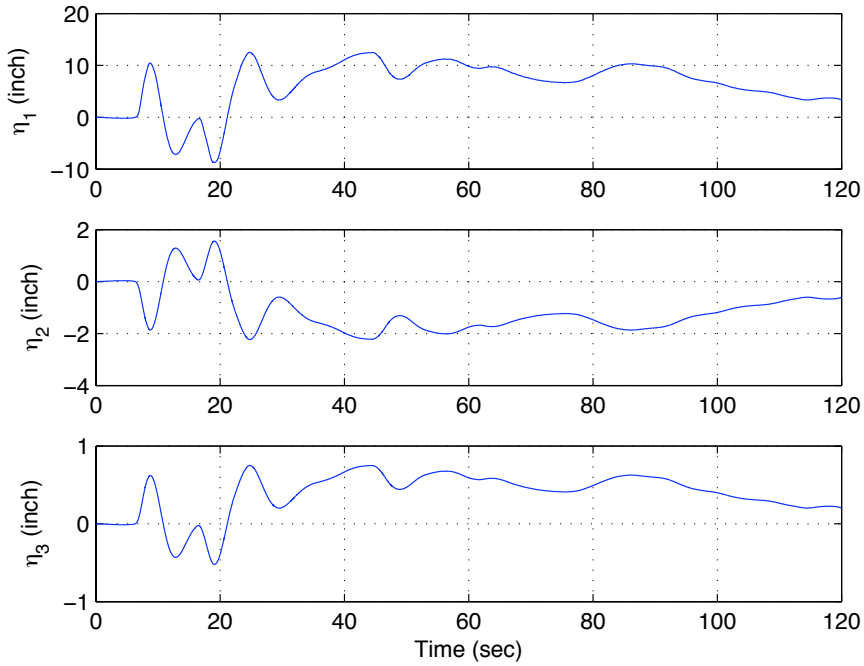

Figure 17. Flexible modes η_1, η_2, and η_3. Note that the higher-frequency components of flexible-mode vibrations cannot be seen in this plot because the flexibl modes are persistently but slowly excited by gimbal contol deflection.

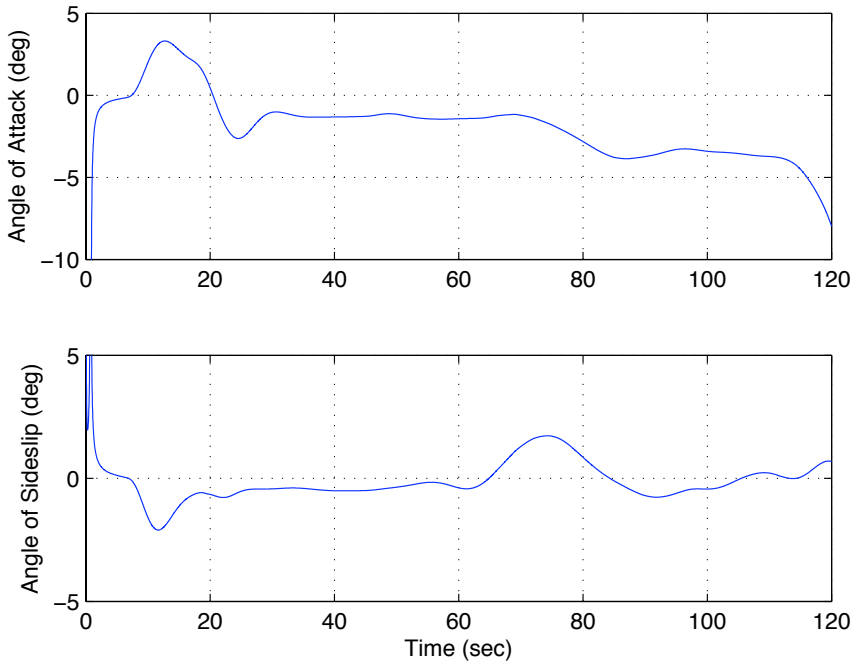

Figure 18. Angle of attack α and angle of sideslip β.

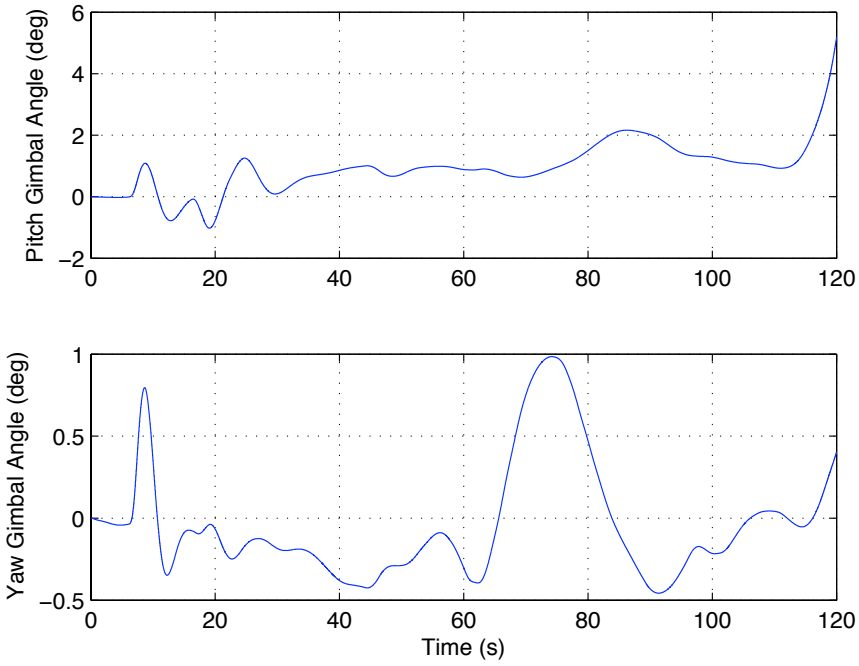

Figure 19. Pitch gimbal angle δ_y and yaw gimbal angle δ_z.

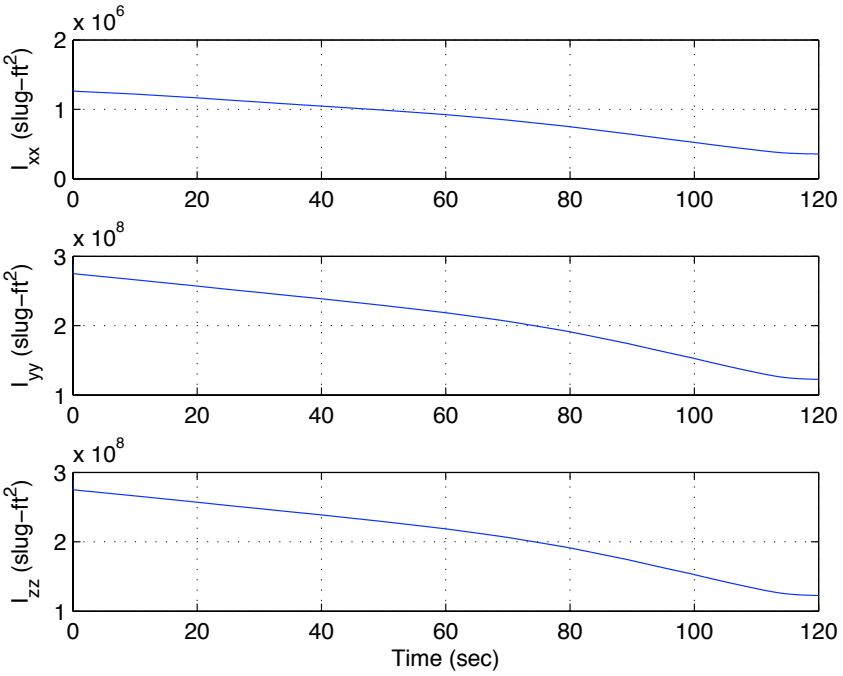

Figure 20. Moments of inertia about the center of gravity.

$$\Delta\dot{q_2} = \frac{1}{2}(q_{3c}\Delta p + q_{4c}\Delta q - q_{1c}\Delta r - r_0\Delta q_1 + p_0\Delta q_3 + q_0\Delta q_4) \tag{73}$$

$$\Delta\dot{q_3} = \frac{1}{2}(-q_{2c}\Delta p + q_{1c}\Delta q + q_{4c}\Delta r + q_0\Delta q_1 - p_0\Delta q_2 + r_0\Delta q_4) \tag{74}$$

$$\Delta\dot{q_4} = \frac{1}{2}(-q_{1c}\Delta p - q_{2c}\Delta q - q_{3c}\Delta r - p_0\Delta q_1 - q_0\Delta q_2 - r_0\Delta q_3) \tag{75}$$

Linearization of the aerodynamic forces and moments:

$$\begin{pmatrix} \Delta F_{aero.xb} \\ \Delta F_{aero.yb} \\ \Delta F_{aero.zb} \end{pmatrix} = \begin{pmatrix} 0 & 0 & 0 \\ 0 & C_{Y\beta}Q_0S/V_m & 0 \\ 0 & 0 & -C_{N\alpha}Q_0S/V_{m.xb} \end{pmatrix} \begin{pmatrix} \Delta u \\ \Delta v \\ \Delta w \end{pmatrix} \tag{76}$$

$$\begin{aligned} \begin{pmatrix} \Delta T_{aero.xb} \\ \Delta T_{aero.yb} \\ \Delta T_{aero.zb} \end{pmatrix} &= \begin{pmatrix} 0 & c_z & -c_y \\ -c_z & 0 & -X_a + c_x \\ c_y & X_a - c_x & 0 \end{pmatrix} \begin{pmatrix} \Delta F_{aero.xb} \\ \Delta F_{aero.yb} \\ \Delta F_{aero.zb} \end{pmatrix} \\ &+ \begin{pmatrix} 0 & 0 & 0 \\ 0 & 0 & C_{Mp\alpha}Q_0Sb/V_{m.xb} \\ 0 & C_{my\beta}Q_0Sb/V_m & 0 \end{pmatrix} \begin{pmatrix} \Delta u \\ \Delta v \\ \Delta w \end{pmatrix} \end{aligned} \tag{77}$$

Linearization of α and β:

$$\Delta\alpha = \frac{1}{V_{m.xb}}\Delta w \tag{78}$$

$$\Delta\beta = \frac{1}{V_m}\Delta v \tag{79}$$

Linearization of the thrust force and moment:

$$\begin{pmatrix} \Delta F_{rkt.xb} \\ \Delta F_{rkt.yb} \\ \Delta F_{rkt.zb} \end{pmatrix} = \begin{pmatrix} 0 \\ -T\Delta\delta_z \\ T\Delta\delta_y \end{pmatrix} \tag{80}$$

$$\begin{pmatrix} \Delta T_{rkt.xb} \\ \Delta T_{rkt.yb} \\ \Delta T_{rkt.zb} \end{pmatrix} = \begin{pmatrix} 0 & c_z & -c_y \\ -c_z & 0 & -X_g + c_x \\ c_y & X_g - c_x & 0 \end{pmatrix} \begin{pmatrix} \Delta F_{rkt.xb} \\ \Delta F_{rkt.yb} \\ \Delta F_{rkt.zb} \end{pmatrix} \tag{81}$$

Quaternion errors:

$$\begin{pmatrix} q_{1e} \\ q_{2e} \\ q_{3e} \\ q_{4e} \end{pmatrix} = \begin{pmatrix} q_{4c} & q_{3c} & -q_{2c} & -q_{1c} \\ -q_{3c} & q_{4c} & q_{1c} & -q_{2c} \\ q_{2c} & -q_{1c} & q_{4c} & -q_{3c} \\ q_{1c} & q_{2c} & q_{3c} & q_{4c} \end{pmatrix} \begin{pmatrix} \Delta q_1 \\ \Delta q_2 \\ \Delta q_3 \\ \Delta q_4 \end{pmatrix} \tag{82}$$

C. Linear State-Space Equations

A linearized state-space model of a rigid vehicle is described by

$$\begin{aligned} \dot{\mathbf{x}} &= \mathbf{A}\mathbf{x} + \mathbf{B}\mathbf{u} \\ \mathbf{y} &= \mathbf{C}\mathbf{x} \end{aligned} \tag{83}$$

where $\mathbf{x} = (\Delta u,\ \Delta v,\ \Delta w,\ \Delta p,\ \Delta q,\ \Delta r,\ \Delta q_1,\ \Delta q_2,\ \Delta q_3,\ \Delta q_4)^T$, $\mathbf{u} = (\Delta T_{rcs},\ \Delta\delta_y,\ \Delta\delta_z)^T$, $\mathbf{y} = (2q_{1e},\ 2q_{2e},\ 2q_{3e},\ p,\ q,\ r)^T$,

$$\mathbf{A} = \left(\begin{array}{c|c|c} \mathbf{A}_{11} & \mathbf{A}_{12} & \mathbf{A}_{13} \\ \hline \mathbf{A}_{21} & \mathbf{A}_{22} & 0 \\ \hline 0 & \mathbf{A}_{32} & \mathbf{A}_{33} \end{array}\right) \tag{84}$$

$$\mathbf{A}_{11} = \begin{pmatrix} 0 & r_0 & -q_0 \\ -r_0 & C_{Y\beta}Q_0S/(mV_m) & p_0 \\ q_0 & -p_0 & -C_{N\alpha}Q_0S/(mV_{m.xb}) \end{pmatrix} \tag{85}$$

$$\mathbf{A}_{12} = \begin{pmatrix} 0 & -w_0 & v_0 \\ w_0 & 0 & -u_0 \\ -v_0 & u_0 & 0 \end{pmatrix} \tag{86}$$

$$\mathbf{A}_{13} = \begin{pmatrix} (2g_yq_{2c} + 2g_zq_{3c}) & (-4g_xq_{2c} + 2g_yq_{1c} - 2g_zq_{4c}) & (-4g_xq_{3c} + 2g_yq_{4c} + 2g_zq_{1c}) & (2g_yq_{3c} - 2g_zq_{2c}) \\ (2g_xq_{2c} - 4g_yq_{1c} + 2g_zq_{4c}) & (2g_xq_{1c} + 2g_zq_{3c}) & (-2g_xq_{4c} - 4g_yq_{3c} + 2g_zq_{2c}) & (-2g_xq_{3c} + 2g_zq_{1c}) \\ (2g_xq_{3c} - 2g_yq_{4c} - 4g_zq_{1c}) & (2g_xq_{4c} + 2g_yq_{3c} - 4g_zq_{2c}) & (2g_xq_{1c} + 2g_yq_{2c}) & (2g_xq_{2c} - 2g_yq_{1c}) \end{pmatrix} \tag{87}$$

$$\mathbf{A}_{21} = \begin{pmatrix} I_{xx} & 0 & 0 \\ 0 & I_{yy} & 0 \\ 0 & 0 & I_{zz} \end{pmatrix}^{-1} \begin{pmatrix} 0 & 0 & 0 \\ 0 & 0 & \left[-\frac{(-X_a+c_x)C_{N\alpha}Q_0S}{V_{m.xb}} + \frac{C_{Mp\alpha}Q_0Sb}{V_{m.xb}}\right] \\ 0 & \left[-\frac{(X_a+c_x)C_{Y\beta}Q_0S}{V_m} + \frac{C_{my\beta}Q_0Sb}{V_m}\right] & 0 \end{pmatrix} \tag{88}$$

$$\mathbf{A}_{22} = \begin{pmatrix} I_{xx} & 0 & 0 \\ 0 & I_{yy} & 0 \\ 0 & 0 & I_{zz} \end{pmatrix}^{-1} \begin{pmatrix} 0 & r_0I_{yy} + I_{zz}r_0 & I_{yy}q_0 - q_0I_{zz} \\ -r_0I_{yy} + I_{zz}r_0 & 0 & -I_{xx}p_0 + p_0I_{zz} \\ q_0I_{xx} - I_{yy}q_0 & I_{xx}p_0 - p_0I_{yy} & 0 \end{pmatrix} \tag{89}$$

$$\mathbf{A}_{32} = \frac{1}{2}\begin{pmatrix} q_{4c} & -q_{3c} & q_{2c} \\ q_{3c} & q_{4c} & -q_{1c} \\ -q_{2c} & q_{1c} & q_{4c} \\ -q_{1c} & -q_{2c} & -q_{3c} \end{pmatrix} \tag{90}$$

$$\mathbf{A}_{33} = \frac{1}{2}\begin{pmatrix} 0 & r_0 & -q_0 & p_0 \\ -r_0 & 0 & p_0 & q_0 \\ q_0 & -p_0 & 0 & r_0 \\ -p_0 & -q_0 & -r_0 & 0 \end{pmatrix} \tag{91}$$

$$\mathbf{B} = \begin{pmatrix} \mathbf{B}_1 \\ \mathbf{B}_2 \\ 0 \end{pmatrix} \tag{92}$$

$$\mathbf{B}_1 = \begin{pmatrix} 0 & 0 & 0 \\ 0 & 0 & -T/m \\ 0 & T/m & 0 \end{pmatrix} \tag{93}$$

$$\mathbf{B}_2 = \begin{pmatrix} I_{xx} & 0 & 0 \\ 0 & I_{yy} & 0 \\ 0 & 0 & I_{zz} \end{pmatrix}^{-1} \begin{pmatrix} 1 & -c_y T & -c_z T + c_y T \\ 0 & (c_x - X_a)T & 0 \\ 0 & 0 & (\mathrm{c}_x - X_a)T \end{pmatrix} \tag{94}$$

$$\mathbf{C} = \begin{pmatrix} 0 & 0 & 0 & 0 & 0 & 0 & 2q_{4c} & 2q_{3c} & -2q_{2c} & -2q_{1c} \\ 0 & 0 & 0 & 0 & 0 & 0 & -2q_{3c} & 2q_{4c} & 2q_{1c} & -2q_{2c} \\ 0 & 0 & 0 & 0 & 0 & 0 & 2q_{2c} & -2q_{1c} & 2q_{4c} & -2q_{3c} \\ 0 & 0 & 0 & 1 & 0 & 0 & 0 & 0 & 0 & 0 \\ 0 & 0 & 0 & 0 & 1 & 0 & 0 & 0 & 0 & 0 \\ 0 & 0 & 0 & 0 & 0 & 1 & 0 & 0 & 0 & 0 \end{pmatrix} \tag{95}$$

VI. Linear Flexible-Body Model

The linear state-space equation of the Ares-I including the flexible-body modes is described by

$$\begin{aligned} \dot{\mathbf{x}} &= \hat{\mathbf{A}}\mathbf{x} + \hat{\mathbf{B}}\mathbf{u} \\ \mathbf{y} &= \hat{\mathbf{C}}\mathbf{x} \end{aligned} \tag{96}$$

where $\mathbf{x} = (\Delta u,\ \Delta v,\ \Delta w,\ \Delta p,\ \Delta q,\ \Delta r,\ \Delta q_1,\ \Delta q_2,\ \Delta q_3,\ \Delta q_4,\ \eta_1,\ \eta_2,\ \eta_3,\ \eta_4,\ \eta_5,\ \eta_6,\ \dot{\eta}_1,\ \dot{\eta}_2,\ \dot{\eta}_3,\ \dot{\eta}_4,\ \dot{\eta}_5,\ \dot{\eta}_6)^T$, and

$$\hat{\mathbf{A}} = \left(\begin{array}{c|cc} \mathbf{A} & \multicolumn{2}{c}{0} \\ \hline 0 & 0 & \boldsymbol{I} \\ & -\boldsymbol{\Omega}^2 & -2\zeta\boldsymbol{\Omega} \end{array}\right) \tag{97}$$

$$\hat{\mathbf{B}} = \left(\begin{array}{c} \mathbf{B} \\ \hline 0 \\ \hline \boldsymbol{\Phi}^T m \mathbf{B}_1 \end{array}\right) \tag{98}$$

$$\hat{\mathbf{C}} = \left(\begin{array}{cccccccccc|c|c} 0 & 0 & 0 & 0 & 0 & 0 & 2q_{4c} & 2q_{3c} & -2q_{2c} & -2q_{1c} & & \\ 0 & 0 & 0 & 0 & 0 & 0 & -2q_{3c} & 2q_{4c} & 2q_{1c} & -2q_{2c} & \boldsymbol{\Psi} & 0 \\ 0 & 0 & 0 & 0 & 0 & 0 & 2q_{2c} & -2q_{1c} & 2q_{4c} & -2q_{3c} & & \\ \hline & & & 0 & 0 & 0 & 1 & 0 & 0 & 0 & 0 & 0 & \\ & & & 0 & 0 & 0 & 0 & 1 & 0 & 0 & 0 & 0 & \boldsymbol{\Psi} \\ & & & 0 & 0 & 0 & 0 & 0 & 1 & 0 & 0 & 0 & \end{array}\right) \tag{99}$$

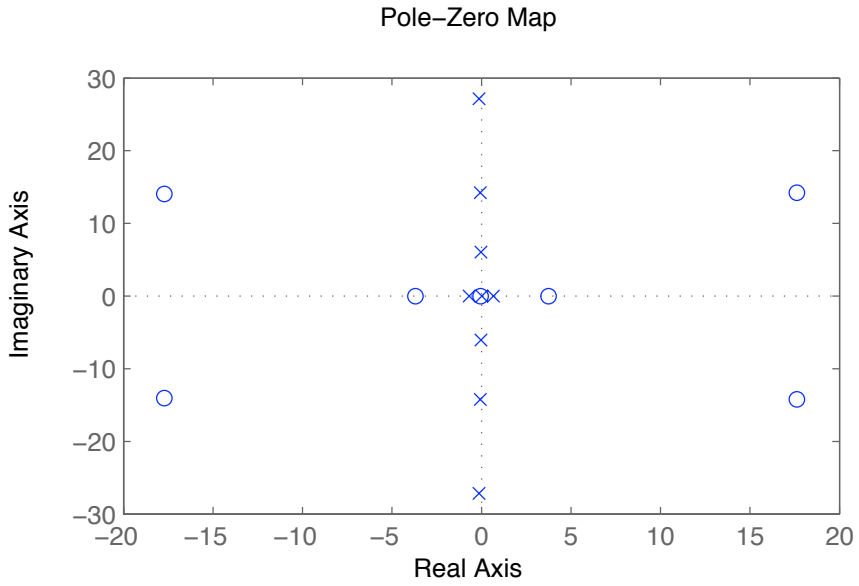

Figure 21. Pitch transfer function model of a reference model of the Ares-I CLV.

A pitch transfer function model of an Ares-I reference model at $t = 60$ sec is found as

$$\frac{2q_{2e}(s)}{\delta_y(s)} = \frac{-0.8589(s+0.043)(s+3.68)(s-3.75)(s^2-35s+512)(s^2+35s+512)}{(s+0.69)(s-0.015)(s-0.66)(s^2+0.06s+36)(s^2+0.14s+202)(s^2+0.27s+738)} \tag{100}$$

The poles and zeros of this pitch transfer function are illustrated in Fig. 21. Such a pole-zero pattern is of typical for flexible vehicles with non-collocated actuator and sensor. Flight control design and analysis of the Ares-I, based on this pitch transfer function model, is presented in [12].

VII. Conclusions

A set of dynamic models of the Ares-I Crew Launch Vehicle, incorporating its propulsion, aerodynamics, guidance and control, and structural flexibility, has been described in this paper. The preliminary results of developing a Matlab-based simulation and linearization program by utilizing NASA's SAVANT Simulink-based program have been discussed. The study purpose was to develop an independent validation tool for the performance and stability analysis of the ascent flight control system of the Ares-I. A linearized model of the Ares-I was obtained as a test case of an independent validation of the ascent flight control design and analysis of the Ares-I.

References

[1] Whorton, M., Hall, C., and Cook, S., "Ascent Flight Control and Structural Interaction for the Ares-I Crew Launch Vehicle," AIAA 2007-1780, April 2007.
[2] Betts, K. M., Rutherford, R. C., McDuffie, J., Johnson, M. D., Jackson, M., and Hall, C., "Time Domain Simulation of the NASA Crew Launch Vehicle," AIAA 2007-6621, August 2007.
[3] Betts, K. M., Rutherford, R. C., McDuffie, J., Johnson, M. D., Jackson, M., and Hall, C., "Stability Analysis of the NASA Ares-I Crew Launch Vehicle Control System," AIAA 2007-6776, August 2007.
[4] James, R. L., "A Three-Dimensional Trajectory Simulation Using Six Degrees of Freedom with Arbitrary Wind", NASA TN D-641, 1961.
[5] Harris, R. J., "Trajectory Simulation Applicable to Stability and Control Studies of Large Multi-Engine Vehicles", NASA TN D-1838, 1963.

[6] Greensite, A. L., "Analysis and Design of Space Vehicle Flight Control Systems," Spartan Books, New York, 1970.
[7] Zipfel, P. H., *Modeling and Simulation of Aerospace Vehicle Dynamics*, AIAA Education Series, 1998.
[8] Wie, B., *Space Vehicle Dynamics and Control*, AIAA Education Series, 1998.
[9] Jang, J.-W., Bedrossian, N., Hall, R., Norris, H., Hall, C., and Jackson, M., "Initial Ares-I Bending Filter Design," AAS 2007-059, February 2007.
[10] Jang, J.-W., Bedrossian, N., and Hall, R., "Ares-I Bending Filter Design Using a Constrained Optimization Approach," AIAA 2008-6289, *AIAA Guidance, Navigation, and Control Conference*, Honolulu, Hawaii, August 18-21, 2008.
[11] Hall, C., Lee, M., Jackson, M., West, M., Whorton, M., and Brandon, J., "Ares-I Flight Control System Overview," AIAA 2008-6287, *AIAA Guidance, Navigation, and Control Conference*, Honolulu, Hawaii, August 18-21, 2008.
[12] Wie, B., Du, W., and Whorton, M., "Analysis and Design of Launch Vehicle Flight Control Systems," AIAA 2008-6291, *AIAA Guidance, Navigation, and Control Conference*, Honolulu, Hawaii, August 18-21, 2008.